Title

Expression of SPARC during development of the chicken chorioallantoic membrane: evidence for regulated proteolysis in vivo.

Journal

Molecular Biology of the Cell, 6(3)

ISSN

1059-1524

Authors

Iruela-Arispe, ML
Lane, TF
Redmond, D
et al.

Publication Date

1995-03-01

DOI

10.1091/mbc.6.3.327

Peer reviewed

Molecular Biology of the Cell
Vol. 6, 327–343, March 1995

Expression of SPARC during Development of the Chicken Chorioallantoic Membrane: Evidence for Regulated Proteolysis In Vivo

M. Luisa Iruela-Arispe,*† Timothy F. Lane,*‡ David Redmond,* Maureen Reilly,§ Robert P. Bolender,* Terrance J. Kavanagh,§ and E. Helene Sage*¶

*Departments of Biological Structure and §Medicine and Environmental Health, University of Washington School of Medicine, Seattle, Washington 98195

Submitted December 8, 1994; Accepted February 13, 1994
Monitoring Editor: Carl-Henrik Heldin

SPARC is a secreted glycoprotein that has been shown to disrupt focal adhesions and to regulate the proliferation of endothelial cells in vitro. Moreover, peptides resulting from the proteolysis of SPARC exhibit angiogenic activity. Here we describe the temporal synthesis, turnover, and angiogenic potential of SPARC in the chicken chorioallantoic membrane. Confocal immunofluorescence microscopy revealed specific expression of SPARC protein in endothelial cells, and significantly higher levels of SPARC were observed in smaller newly formed blood vessels in comparison to larger, developmentally older vessels. SPARC mRNA was detected at the earliest stages of chorioallantoic membrane morphogenesis and reached maximal levels at day 13 of embryonic development. Interestingly, steady-state levels of SPARC mRNA did not correlate directly with protein accumulation; moreover, the protein appeared to undergo limited degradation during days 10–15. Incubation of [^{125}I]-SPARC with chorioallantoic membranes of different developmental ages confirmed that extracellular proteolysis occurred during days 9–15, but not at later stages (e.g., days 17–21). Comparison of peptides produced by incubation with chorioallantoic membranes with those generated by plasmin showed an identical pattern of proteolysis. Plasmin activity was present throughout development, and in situ zymography identified sites of plasminogen activator activity that corresponded to areas exhibiting high levels of SPARC expression. Synthetic peptides from a plasmin-sensitive region of SPARC, between amino acids 113–130, stimulated angiogenesis in the chorioallantoic membrane in a dose-dependent manner; in contrast, intact SPARC was inactive in similar assays. We have shown that SPARC is expressed in endothelial cells of newly formed blood vessels in a manner that is both temporally and spatially restricted. Between days 9 and 15 of chorioallantoic membrane development, the protein undergoes proteolytic cleavage that is mediated, in part, by plasmin. SPARC peptides released specifically by plasmin induce angiogenesis in vivo. We therefore propose that SPARC acts as an intrinsic regulator of angiogenesis in vivo.

INTRODUCTION

SPARC is a secreted glycoprotein synthesized by a variety of cells involved in morphogenesis and remodeling (reviewed by Lane and Sage, 1994). Although high levels are found in bone, somites, and platelets (Otsuka *et al.*, 1984; Stenner *et al.*, 1986; Holland *et al.*, 1987; Sage *et al.*, 1989a), a greater number of cell types express the protein in vitro, as part of a response termed "culture shock" (Sage *et al.*, 1984). SPARC binds to extracellular matrix components such as

† Current address: Department of Pathology, Harvard Medical School and Beth Israel Hospital, 330 Brookline Ave., Boston, MA 02215.

‡ Current address: Department of Genetics, Harvard Medical School, 200 Longwood Ave., Boston, MA 02115.

¶ Corresponding author: Department of Biological Structure, SM-20, University of Washington, Seattle, WA 98195.

thrombospondin (Clezardin *et al.*, 1988), collagens I, III, and IV, and V (Sage *et al.*, 1989b; Mayer *et al.*, 1991), and PDGF-B chain (Raines *et al.*, 1992). Consistent with a role in remodeling tissues, expression of SPARC mRNA and protein has been noted in endothelial cells as part of angiogenesis during development and wound repair (Reed *et al.*, 1993; Lane *et al.*, 1994). In vitro, SPARC is significantly increased during the organization of endothelial cords and tubes (Iruela-Arispe *et al.*, 1991a,b) and appears to regulate endothelial cell shape and proliferation (Sage *et al.*, 1989b; Funk and Sage, 1991, 1993). Although an association with angiogenesis has been apparent from these and other studies, an understanding of the role of SPARC in this process has remained elusive.

Angiogenesis is a complex process that leads to an increase in vessel density during development, in tissue remodeling, and in response to factors released by tumors and anoxic tissues. It comprises a series of modifications in endothelial cell behavior that lead to the acquisition of an invasive phenotype. After endothelial cell stimulation, successive changes in cell shape, migration, and proliferation result in the morphogenesis of capillary networks. Invasion is facilitated by an increase in the levels of local proteases, particularly plasmin/plasminogen activator (PA)[1] and metalloproteases (Pepper and Montesano, 1990). Angiogenic growth is eventually curtailed by decreased levels of stimulators or by specific inhibitors, and is characterized by a return to the noninvasive and mitotically quiescent state (Folkman and Klagsbrun, 1987). An understanding of endothelial cell activation, as well as the elements that regulate each of the cellular events involved in vessel formation, is relevant to the control of several pathologies, including cancer.

Among the systems available for the study of angiogenesis in vivo, the chicken chorioallantoic membrane (CAM) provides advantages such as a relatively simple structure, fast growth, and accessibility. The CAM develops as a diverticulum of the endoderm 48 h after fertilization and reaches a diameter of 9 cm in 7 days. Vascularization of the CAM arises from progressive endothelial cell proliferation (Ausprunk *et al.*, 1974) and capillary branching that expands radially. Since the vessels near the center are formed first, they are developmentally older than the vessels near the edges of the expanding membrane.

In this study, we found that SPARC was expressed at high levels during the development of the CAM at periods coincident with capillary branching and growth; however, proteolysis was also observed at specific times during development. Degradation was not apparent after day 17, when capillary morphogenesis had essentially ceased. High steady-state levels of mRNA correlated with maximum proteolysis. Because the degradation of SPARC by plasmin and by a 15-d CAM were highly similar, and a previous study had shown that cleavage of SPARC by plasmin resulted in the release of angiogenic peptides (Lane *et al.*, 1994), we quantified the angiogenic activity of these fragments in the CAM. Peptides from basic region II (amino acids 113–130) induced capillary growth in a dose-dependent manner, whereas peptides from other regions were without effect. Intact SPARC did not promote an angiogenic response.

Our data indicate that the degradation of SPARC in the extracellular milieu could result in the release of bioactive peptides; moreover, maximal levels of plasmin appeared to coincide with SPARC degradation. Collectively, these results implicate SPARC as a regulator of angiogenesis and provide evidence that the plasmin/PA system might act, in part, to regulate its activity in vivo.

MATERIALS AND METHODS

Animals and Tissue Culture

Fertilized white Leghorn chicken eggs (Biological Supply, Lynnwood, WA) were incubated at 37°C in 60% relative humidity. At day 3, eggs were opened into petri dishes. Embryos with intact CAMs and yolks were cultured under sterile conditions in an humidified tissue culture incubator at 37°C, 1–3% CO_2, essentially as described by Auerbach *et al.* (1974).

Antibodies

Rabbit polyclonal IgG generated against a peptide sequence from the carboxy-terminus (amino acids 254–273) of murine SPARC (anti-4.2; NH_2-TCDLDNDKYIALEEWAGCFG) (Lane and Sage, 1990) was used for both immunohistochemistry and immunoblot analysis of chicken SPARC. The chicken sequence is 85% identical to the mouse over this region, and the antibodies have been shown to recognize the chicken protein (Bassuk *et al.*, 1993). Antibodies used for mapping of human SPARC degradation products included a rabbit polyclonal IgG against intact murine SPARC (Sage *et al.*, 1989a), and an antiserum against a synthetic peptide of SPARC (amino acids 113–130) (Table 1).

Protein Extraction and Purification

CAMs were allowed to develop in ovo at 37°C. Two to four eggs were harvested per day to obtain multiple samples from day 3 to 21 of development. After isolation, CAMs were extracted in 10 volumes of extraction buffer (50 mM Tris-HCl, pH 7.6, 0.4% NP-40), at 4°C, with a Polytron tissue homogenizer (Brinkmann Instruments, Westbury, NY). The extraction buffer contained the following proteinase inhibitors: 1 μg/ml leupeptin, 1 μg/ml pepstatin A, 10 mM NEM (Sigma Chemical, St. Louis, MO), 2 mM phenylmethylsulfonyl fluoride (PMSF) (Sigma Chemical), 2 mM 1,10-phenanthroline (Sigma Chemical, 0.1 mM *N*-tosyl-L-lysine chloromethyl ketone (Sigma Chemical), and 0.2 mM *N*-tosyl-L-phenylalanine chloromethyl ketone (Sigma Chemical). The last three inhibitors were diluted directly into the sample during homogenization. Homogenates were allowed to stand for 10 min at 4°C. Insoluble material was removed by centrifugation at 12,000 rpm in a microfuge for 5 min at 4°C. The resulting supernates were stored at −70°C. Isolation of CAMs was

[1]Abbreviations used: CAM, chorioallantoic membrane; PA, plasminogen activator.

Table 1. Sequences of synthetic peptides

Name	Sequence[a]	Mass[b]
1. 4–23	QTEVAEEIVEEETVVEETGV	2219.3
2. 54–73	CQNHHCKHGKVCELDESNTP	2279.5
3. 113–130	TLEGTKKGHKLHLDYIG	1910.2
4. $113–130_{H121-R}$	TLEGTKKGrKLHLDYIG	1938.2
5. $113–130_{K119-A}$	TLEGTKaGHKLHLDYIG	1853.1
6. 119–122	KGHK	469.3
7. 120–122	GHK	341.2

[a]Peptides were named according to their position within the published sequence of murine SPARC after the removal of the signal sequence (Mason *et al.*, 1986). Amino acid residues are indicated by single letter code. Mutations in peptides are indicated by a subscript in the name and by a lower-case letter in the sequence.

[b]Mass (in D) was calculated with the aid of the MacProMass program.

always performed at the same time of day to ensure consistent timing of developmental stages.

CAM extracts were dialyzed against DE buffer (50 mM Tris-HCl, pH 8.0, 4 M urea) for 24 h at 4°C. Insoluble material was removed by centrifugation as above, and the samples were applied to individual minicolumns that contained DE-52 anion-exchange resin (Whatman, Hillsboro, OR) previously equilibrated in DE buffer. The resin was washed with 4-column volumes of DE buffer to remove unbound material (this fraction was referred to as DE-0). Bound proteins were eluted stepwise by application of buffers containing increasing concentrations of NaCl: 75 mM NaCl (DE-I), 175 mM (DE-II), and 500 mM NaCl (DE-III). Fractions were dialyzed against H_20 and lyophilized before analysis.

Sodium Dodecyl Sulfate-Polyacrylamide Gel Electrophoresis (SDS-PAGE) and Immunoblotting

CAM extracts and anion-exchange fractions were resolubilized in 50 mM Tris-HCl, pH 7.5, containing 150 mM NaCl and 1 mM $CaCl_2$. Protein concentrations were determined with a Bradford protein assay kit (Pierce, Rockford, IL) and a calibrated solution of bovine serum albumin (BSA). Equivalent amounts of protein (600 μg of unfractionated proteins or 200 μg of each ion-exchange fraction) were separated by SDS-PAGE and transferred to nitrocellulose membranes for immunoblot analysis. For SDS-PAGE, peptides were solubilized in sample buffer (Laemmli, 1970), heated at 95°C for 3 min in the presence of 5 mM dithiothreitol (DTT), and separated on 10–20% gradient minigels (Integrated Separation Systems, Natick, MA) with a tricine-SDS buffer system (Schägger and von Jagow, 1987). Proteins resolved by SDS-PAGE were transferred to nitrocellulose, visualized by exposure to amido black, and photographed. Nonspecific binding was blocked with MT-buffer (phosphate-buffered saline [PBS], pH 7.7, containing 1% nonfat dried milk and 0.05% Tween-20). Blots were subsequently incubated with anti-SPARC antibodies for 2 h at room temperature, followed by 0.05 mCi/ml [^{125}I]-protein A (Dupont NEN, Boston, MA). Radiolabeled complexes were detected as autoradiographic images on x-ray film exposed at −70°C with two intensifying screens (Kodak, Rochester, NY). Molecular weight was determined by reference to the migration of characterized standards (Life Technologies, Bethesda, MD): myosin (200,000), phosphorylase B (97,400), BSA (68,000), ovalbumin (43,000), carbonic anhydrase (29,000), β-lactoglobulin (18,400), and lysozyme (14,300).

Northern Blot Analysis

CAMs from days 4–19 of development were isolated from embryos, rinsed in Dulbecco's modified Eagle's medium (DME), minced, and subjected to an RNA extraction procedure. Total RNA was purified, fractionated by electrophoresis on a 1.2% denaturing agarose gel, transferred to Nytran membranes by vacuum blotting, and prehybridized for 3–5 h as previously described (Iruela-Arispe *et al.*, 1993). A chicken SPARC cDNA probe (Bassuk *et al.*, 1993) was radiolabeled with [^{32}P]dCTP ($0.2–0.5 \times 10^9$ cpm/μg DNA) and purified by chromatography on Sephadex minicolumns (Pharmacia, Piscataway, NJ). The probe was added to the prehybridization solution, and hybridization proceeded at 42°C for 12–18 h. Blots were also hybridized with a 28 S rRNA probe to control for loading and transfer efficiency (Iruela-Arispe *et al.*, 1991a). For quantification, all values were normalized to the 28 S rRNA signal.

Whole-mount Immunocytochemistry and Confocal Microscopy

CAMs were dissected, rinsed in DMEM, fixed with 4% paraformaldehyde at 4°C for 4 h, and washed extensively in PBS for several hours. CAMs were incubated with 50 mM DTT for 30 min, washed in PBS, incubated with RNAse A (10 μg/ml) for 10 min, rinsed in PBS, and blocked in a solution containing 1% goat serum and 0.1% Tween-20 in PBS. Tissues were incubated with an affinity-purified rabbit anti-peptide IgG that recognizes SPARC (anti-peptide 4.2) for 4 h at room temperature, washed in blocking solution, incubated with biotinylated anti-rabbit IgG for 4 h at room temperature, washed in blocking solution overnight, and finally incubated with avidin-FITC. After extensive washing, CAMs were stained with propidium iodide (10 μg/ml) for visualization of nuclei. Controls included the use of preimmune serum and preabsorption of the antibody with the immunizing peptide. The preparations were examined on an ACAS 570c Laser Cytometer (Meridian Instruments, Okemos, MI) set in confocal mode. Dual color scans were acquired with 488 nm excitation from a 5 W argon-ion laser (Coherent, Palo Alto, CA). For simultaneous detection of FITC and propidium iodide, the epifluorescent light was separated from the excitation light by a 500 nm dichroic mirror and a 515 nm LP barrier filter. The light was then split with a 575 nm short-pass dichroic filter. FITC fluorescence was further delineated by passage through a 530/30 bandpass filter in front of the first detector. Propidium iodide fluorescence was detected after passage through a 605 nm long-pass filter placed in front of the second detector. Photomultiplier tube voltages were calibrated with a standardized fluorescent plastic slide before each experiment to ensure a linear response with respect to fluorescence intensity.

To improve resolution, we scanned CAMs at several different field sizes. For large-scale scans, the motorized microscope stage was set to scan 180 × 180 pixels with a step size of 10 μ/pixel with a 40 X LWD phase objective (NA = 0.55) and a pinhole size of 225 μm. Smaller areas within different regions of the CAM were scanned similarly at 180 × 180 pixels, but with a smaller step size (0.5 or 2 μ/pixel). For quantification of levels of SPARC in different zones, each CAM was divided into three regions designated as follows: zone I - central, zone II - intermediate, and zone III - peripheral. Images were acquired by random selection of areas within each zone in the CAM. The digitized images were displayed and analyzed with a microcomputer resident in the ACAS 570c, and the dual color image analysis software package provided by the manufacturer. Alternatively, the image files were exported to a Macintosh LC II microcomputer (Apple Computer, Inc., Cupertino, CA) and analyzed with the National Institutes of Health Image software package (version 1.49, National Institutes of Mental Health, Bethesda, MD).

For simultaneous identification of endothelial cells and SPARC, a day 7 chicken embryo was perfused through the left ventricle with Di-acetylated–low density lipoprotein (Ac-LDL) for 2 min. The vas-

culature was flushed with saline for 10 min and was subsequently fixed with 4% paraformaldehyde. After perfusion, the CAM was post-fixed by immersion in 4% paraformaldehyde. Staining for SPARC and visualization by confocal microscopy were performed as described above.

In Situ Digestion of SPARC

Iodination of SPARC was performed by the chloramine-T procedure as described by Yost and Sage (1993). Approximately 1 ng of iodinated protein was placed onto staged CAMs. Preparations were incubated for 9 h at 37°C. A circle of tissue overlapping the area of SPARC application (0.5 cm in diameter) was subsequently dissected from the CAMs, rinsed twice in DMEM, and placed in 500 μl of a solution containing the following proteinase inhibitors: 2 mM PMSF, 10 mM NEM, 5 mM EDTA, 1 μg/ml leupeptin, and 1 mM amiloride. Samples were homogenized with a Dounce homogenizer and were centrifuged for 5 min. The supernates were transferred to a fresh tube, and an aliquot was counted by liquid scintillation spectrometry (Beckman, Palo Alto, CA). Controls included incubation of SPARC alone at 37°C and with CAM tissue in the presence of a solution of proteinase inhibitors containing 2 mM PMSF, 10 mM NEM, 5 mM EDTA, 1 μg/ml leupeptin, 0.1 mM mM *N*-tosyl-L-lysine chloromethyl ketone, 0.2 mM *N*-tosyl-L-phenylalanine chloromethyl ketone, and 1 mM amiloride.

An aliquot of 50,000 cpm was mixed with tricine sample buffer (Schägger and von Jagow, 1987) in the presence of DTT, heated to 95°C for 1 min, and resolved on an SDS-tricine minigel (Integrated Separation Systems). After electrophoresis, the gel was fixed, dried, and exposed to X-AR film (Kodak).

For immunoblot analysis, 5 μg of unlabeled SPARC was placed onto 7-day and 15-day CAMs. The incubation and extraction procedure was identical to that described above. In addition, 5 μg of SPARC was digested with 1 unit of plasmin (Sigma Chemical) for 9 h at 37°C. SPARC alone was also incubated under the same conditions. The samples were subjected to SDS-PAGE, transferred to nitrocellulose, and probed with several anti-SPARC antibodies. Antigen-antibody binding was detected by chemiluminesence (Bio-Rad, Hercules, CA), after incubation with an alkaline phosphatase-labeled secondary antibody.

Measurement of Plasmin

Whole CAMs from days 4–17 were dissected, rinsed in DME, and homogenized in the absence of proteinase inhibitors in 50 mM Tris-HCl (pH 7.5), containing 100 mM NaCl and 1 mM $CaCl_2$, in a Polytron apparatus. One aliquot from each sample was used for measurements of protein concentration by a Bradford assay (Pierce). Plasmin concentration was measured in microtiter plates by the addition of 100 μl of the chromogenic substrate S2304 (stock solution of 4 mM) (Kabi Pharmaceuticals, Franklin, OH) to equivalent amounts of protein extract (500 μg). The reactions were incubated at 37°C for 20 min, and absorbance was determined at 490 nm with an automated ELISA plate reader. Purified plasmin was used to generate a standard curve, and absorbance values from homogenates were converted into plasmin concentrations (μg/ml) by interpolation from the standard curve.

In Situ Zymography

CAMs from days 5–17 were dissected, rinsed in DMEM, and placed on a glass surface maintained at 37°C before application of the plasminogen overlay. A suspension consisting of 2% nonfat dry milk in PBS (supernates were collected from an 8% stock solution, heated at 95°C for 30 min, and centrifuged for 15 min at 3,000 × g), 1% melted agarose, and 40 μg/ml purified human plasminogen (Sigma Chemical) was prepared at 50°C (Sappino *et al.*, 1991). The mixture was pipetted carefully over the CAM and allowed to polymerize. The agar jelled immediately and gradually became opalescent. We found that 1 ml was sufficient to cover 2 cm^2 of the CAM. Care was taken in all overlays to ensure that an equal volume, and therefore an equal concentration, of plasminogen was applied per unit area of tissue. Samples were incubated at 37°C in an humidified incubator for 8 h. Lytic activity was visualized as clear zones under dark-field illumination. The first lytic zones usually became visible within 4 h after overlay. The CAMs were photographed under dark-field illumination before and after incubation to document the extent of digestion. Similar experiments were performed without plasminogen or in the presence of 1 mM amiloride (Vassali and Belin, 1987).

Mesh Assay and Quantification of Capillaries

Type I collagen gels containing PBS, SPARC, or SPARC peptides were cast between meshes of an inert, nonantigenic tissue as follows: mesh tissue (Tetko, #3–300/50) was cut into squares of 4 × 4 mm or 2 × 2 mm and was autoclaved. Type I collagen (vitrogen, Celtrix Corp., Palo Alto, CA) was neutralized with 10 × PBS and 0.1 N NaOH and was kept on ice to avoid polymerization. Suspensions were prepared by mixing of the peptides with the neutralized vitrogen. Each mixture (20 μl) was pipetted onto 4 × 4 mm meshes and allowed to polymerize at 37°C. An outer mesh square (2 × 2 mm) was applied to complete the sandwich. The amino acid sequences of the peptides are shown in Table 1. bFGF and BSA were used as positive and negative controls, respectively.

Meshes were applied to day 11 CAMs for 24 h. The meshes were always placed between areas II and III (Figure 1A). After 24 h, the specimens were recovered from the CAM, fixed in paraformaldehyde, and processed for histological examination and morphometry. Vitrogen sandwiches were embedded in paraffin, and 10-μm sections were obtained. Sections were stained with hematoxylin and eosin.

The densities of capillaries (number of capillaries per mm^2) and of endothelial cells in the meshes were measured by an optical volume fractionator method (Bolender, 1993; Bolender and Charleston, 1993) and a computer software program. This software guided the initial experimental design by the provision of a series of simulators based on the volume of the structure and a target minimal error of 0.005%. The principles of this novel stereological procedure are based on the optical dissector (Gundersen *et al.*, 1988) and the fractionator (Gundersen, 1986). With the aid of the optical volume fractionator and the OPTIMAS program, we estimated the total volume of the meshes, the numerical density of the cells, and the total volume of cells/mesh.

Initially, the volume of the polymerized vitrogen was obtained by the Cavalieri method (Gundersen and Jensen, 1987): volume of the mesh analyzed = 0.25 cm^3 (±0.05). The meshes were 2.5–3 mm long and 1.5–2 mm thick.

To quantify the density of capillaries in the meshes, we used a test grid with parameters of Dgrid, 1 cm; Pgrid, 30. This grid allowed us to estimate the area of the sections. The test grid was applied to the monitor screen, and an image of the mesh was projected (total magnification = ×55). Intersecting capillaries were identified by the OPTIMAS program and were counted to obtain the total density of vessels.

Capillary counts were obtained in sections cut through the plane of the mesh; the size of the mesh could therefore be used as an internal standard for measurements of area. The coefficient of error for the capillary density was calculated according to the procedure of Brændgaard *et al.* (1990).

RESULTS

SPARC Protein Is Preferentially Expressed by Endothelial Cells in Newly-formed Regions of the CAM

During development, the CAM displays a progressive gradient of growth that originates from the base of the

allantois. The structure is fully formed by day 15 and provides increased surface area for gas exchange in the embryo. Angiogenesis follows the pattern of CAM growth and thus proceeds from the center toward the periphery. As a result, central vessels are developmentally older than their peripheral counterparts. If SPARC is involved in proliferation or invasion of endothelial cells, a corresponding central-to-peripheral gradient of its expression in the CAM would be expected. To test this prediction, we performed immunohistochemical analysis of SPARC in CAMs isolated between days 8–12 of development. Quantification of SPARC expression was assessed by direct measurements of fluorescence intensity with a laser-activated confocal microscope.

Figure 1A is a camera lucida illustration of a day 10 CAM, divided into three zones that correspond to regions of developmental age. Zone I is the center of the CAM and contains the highest density of large-caliber vessels. Zone III corresponds to the peripheral zone, still expanding at this stage in development, which contains the highest percentage of actively growing capillaries. Between zones I and III, there is a transitional region (zone II) with vessels at intermediate stages of maturation in comparison to zones I and III.

The distribution of SPARC within a CAM is presented in Figures 1 and 2. Confocal analysis of a day-10 CAM revealed SPARC protein associated with endothelial cells in a central-to-peripheral gradient (Figure 1B). In this image, fluorescence intensity (levels of SPARC) has been translated into a color scale, a process that allows discrimination of antigen concentration. Most of the CAM vasculature was visualized as blue or green, an indication that low levels of SPARC were expressed throughout the vasculature. Toward the periphery (zone III), a larger number of vessels were stained, the yellow and red colors indicating higher concentrations of SPARC protein. Examination at higher magnification of cells that were stained with anti-SPARC IgG indicated that endothelial cells were the major site of SPARC synthesis. To verify this observation, we performed a double-label experiment in which the CAM was flushed with Ac-LDL before immunolocalization of SPARC. Endocytosis of Ac-LDL is routinely used for identification of endothelial cells (Yablonka-Reuveini, 1989). Figure 1, C and D shows a 0.5-μm optical slice through a small blood vessel. Two cells (identified by arrows) were stained for both Ac-LDL uptake (Figure 1C) and for SPARC (Figure 1D). Analysis of other regions of these CAMs revealed that virtually all cells that were immunolabeled with SPARC were also labeled with Ac-LDL. In initial immunohistochemical studies of the CAM, it appeared that occasional mesenchymal cells were also stained with anti-SPARC antibodies. However, subsequent studies with Ac-LDL as an endothelial marker showed that most, if not all, of this staining could be attributed to endothelial cells lying just outside the plane of section.

We next quantitatively analyzed the levels of SPARC in vessels of zones I, II, and III. Figure 2 shows a panel of representative confocal images collected from the three different zones defined in Figure 1A. Panels A and B represent images from zone I; panels C and D, images from zone II, and panels E and F, images from zone III. In all the images examined, SPARC was primarily associated with endothelial cells. Blood, inflammatory cells, and the majority of stromal cells were negative (Figure 2, panels B, D, and F). These results are in agreement with observations obtained from the double-labeling experiments. Capillaries from zone III exhibited the highest levels of staining for SPARC (Figure 2F), and virtually all capillary endothelial cells in this zone were immunoreactive. In zone I, capillaries reactive with anti-SPARC IgG were rare. The pattern of expression observed in zones I and II was similar; in both regions, the intensity of staining in endothelial cells was low. When positive cells were identified in vessels from zones I and II, the pattern was interrupted, i.e., not all endothelial cells were positive (Figure 2, B and D). This profile has been observed in vessels from other tissues (Lane *et al.*, 1994). It is therefore conceivable that cells from older vessels display discontinuous expression of SPARC, or that the endothelium is heterogeneous with respect to the synthesis of this protein.

All immunocomplexes detected were associated with discrete cells and appeared to be intracellular. The intensity of intracellular fluorescence resulting from SPARC immunocomplexes was analyzed in endothelial cells from 25 distinct vessels in each zone (Figure 2G). Values were normalized to the level of propidium iodide (corresponding to the number of nuclei per area) in identical areas. The results, shown as a histogram, indicate that endothelial cells from peripheral vessels expressed, on average, four times more SPARC than endothelial cells from older (central) vessels.

Expression of SPARC Correlates with Maximal Capillary Growth

In addition to the radial progression of blood vessel development observed within a CAM, a measure of vessel maturity can be obtained by direct comparison of developmental stages. Previous studies have shown that rates of capillary growth are maximal between days 7–12, and decline steadily thereafter (Ausprunk *et al.*, 1974). We used this developmental sequence to determine the expression of SPARC in relation to the

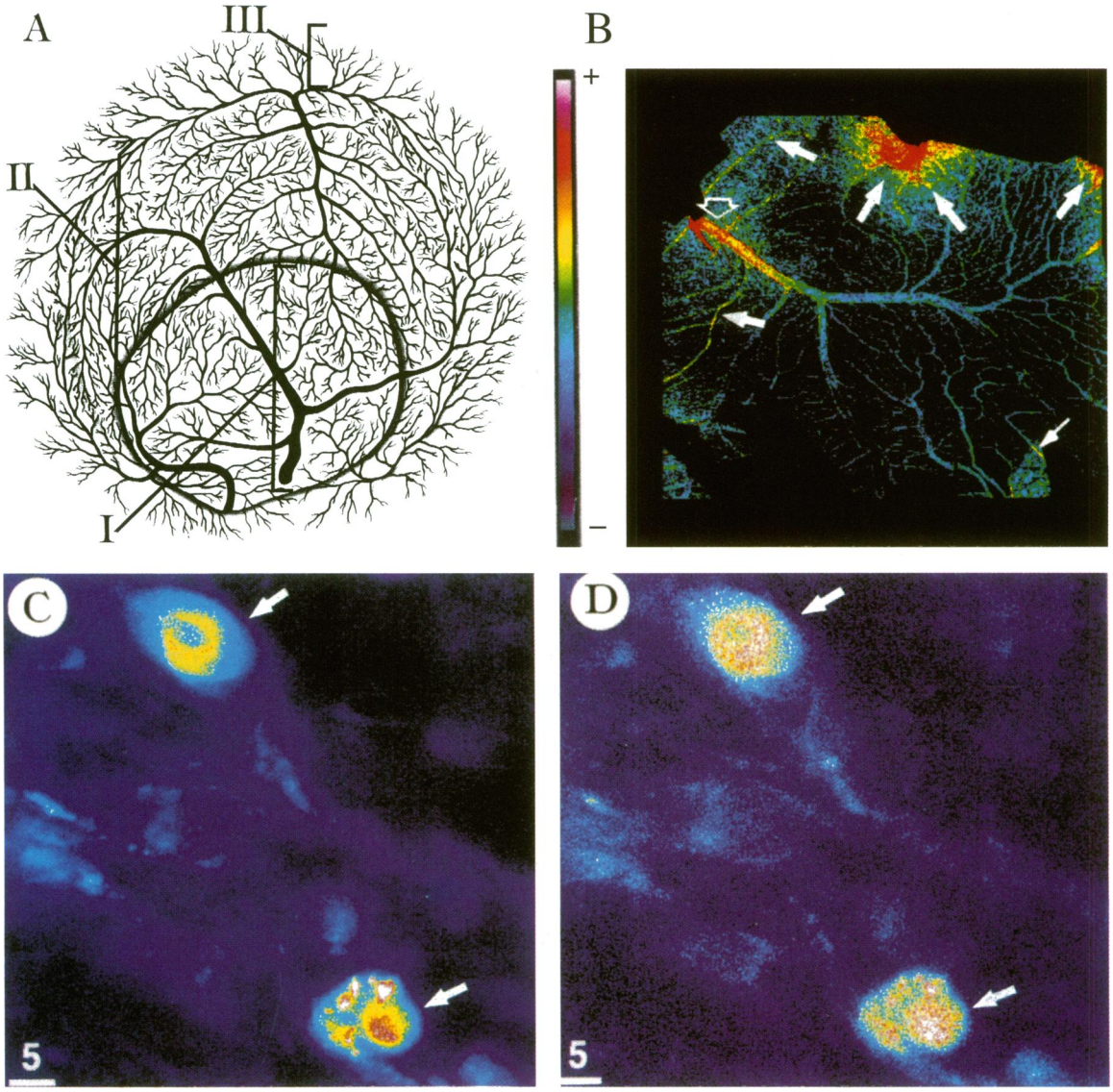

Figure 1. Distribution of SPARC in the CAM. (A) Camera lucida illustration of the vasculature in a day 10 CAM. Progression of angiogenesis follows a centrifugal pattern: vessels in the center (zone I) are, in general, larger and developmentally older than vessels in the periphery (zone III). The intermediate region is designated zone II. (B) Confocal scan of a day 10 CAM after whole mount staining with anti-$SPARC_{254-273}$ peptide antibodies followed by FITC-conjugated secondary antibodies. Fluorescence intensity is represented as a pseudocolor image: a color scale is provided on the left. Highest concentrations of bound antibody are represented in red (+), and lowest concentrations are represented in violet (−). Arrows indicate high levels of expression of SPARC. (C and D) Confocal images from a single blood vessel. The CAM had been perfused with Ac-LDL, an endothelial cell marker, before fixation and staining with anti-$SPARC_{254-273}$ peptide antibodies. (C) CAM visualized for fluorescence due to bound and/or endocytosed Ac-LDL. (D) CAM visualized for fluorescence due to anti-SPARC immunocomplexes. Arrows indicate two cells that are positive for both Ac-LDL and SPARC. Other cells outside the plane of focus can also be identified. Bar in C and D = 5 μm.

degree of angiogenesis and endothelial cell differentiation.

Protein homogenates from CAMs at successive days of development were examined for the presence of SPARC. Initial immunoblots revealed significant levels of protein in extracts from days 7–10; however, detection of SPARC in the total extracts was compromised by high levels of lipid and comigrating protein. To improve the signal, we took advantage of the affinity of SPARC for anion-exchange resins and obtained a partial purification of SPARC before electrophoresis (Sage *et al.*, 1989b). The isolation procedure is shown in Figure 3A. After extensive dialysis, the fractions were separated by SDS-PAGE (Figure 3B), trans-

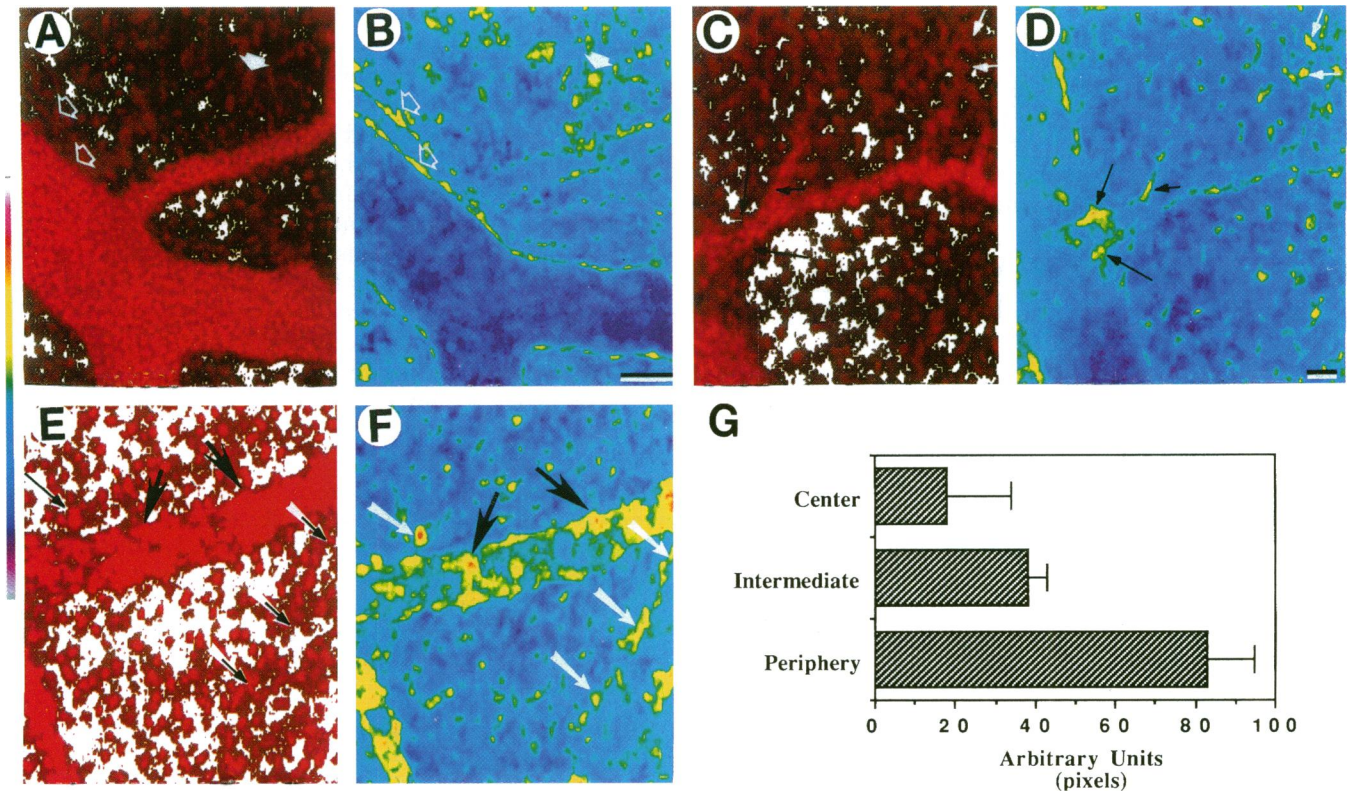

Figure 2. Localization of SPARC in capillaries from the center, intermediate, and peripheral zones of the CAM. (A-F) CAMs were fixed, blocked in PBS/Tween, and incubated with anti-SPARC$_{254-273}$ peptide antibodies followed by FITC-secondary antibody. The CAM preparations were also stained with propidium iodide for identification of nuclei. Confocal images were obtained from the center (A and B), intermediate (C and D), and peripheral zones (E and F). Images corresponding to propidium iodide are panels A, C, and E, and FITC images are panels B, D, and F. Note that images are at different magnifications (designated by bars in the FITC-labeled panels). Arrows indicate identical cells within a pair, stained with propidium iodide and FITC. A scale of fluorescence intensity is provided on the left. Bars = 100 μm. (G) Histogram of SPARC levels in endothelial cells from zones I, II, and III. CAMs from days 8–12 were stained with anti-SPARC$_{254-273}$ peptide antibodies and propidium iodide, as described above. Twenty-five vessels were selected from each zone (center, intermediate, and peripheral), and scanned in confocal mode. The intensity of the FITC signal was normalized to the number of nuclei (propidium iodide signal). These normalized values represent the levels of SPARC/cell. Bars indicate mean intensity ±SEM.

ferred to nitrocellulose, and probed with anti-SPARC antibodies (Figure 3C). Immunoblots showed that SPARC was present in the initial extract (Figure 3C, lane 2) and was eluted from the column with 175 mM NaCl (DE-II fraction, Figure 3C, lane 5).

Protein extracts were obtained from CAMs at days 5–17 of development, purified by ion-exchange chromatography, and assayed for SPARC by immunoblot analysis. Equivalent concentrations of isolated proteins were transferred to nitrocellulose and stained with amido black (Figure 4A), and were subsequently incubated with anti-SPARC antibodies and [^{125}I]-protein A (Figure 4B). Maximal levels of intact SPARC protein were detected at days 7 and 16. Steady-state levels of the protein appeared to diminish progressively between days 8 and 13 (Figure 4B, lanes 5–10) and to increase after day 15 (Figure 4B, lanes 11–12). A specific degradation product of approximately 35 kDa was also identified on immunoblots between days 11–15 (Figure 4B, lanes 8–11). That the antibody is specific for epitopes within a short, C-terminal region of SPARC possibly precluded detection of proteolytic fragments other than the 35-kDa peptide. This pattern was displayed consistently in four independent experiments. One of the isolations was performed in the presence of a 10-fold increase in the concentrations of proteinase inhibitors, with no change in the pattern of cleavage. Because proteinase inhibitors prevented the degradation of an exogenous iodinated SPARC after 6 h of incubation with CAM extracts (unpublished experiments, and see also Figure 7A), proteolysis did not likely result from experimental manipulation of the tissue.

To investigate whether the lower levels of intact SPARC protein from days 8–13 were due to reduced biosynthesis, we analyzed SPARC mRNA production over this interval. SPARC mRNA levels actually increased up to day 13, in concert with the overall

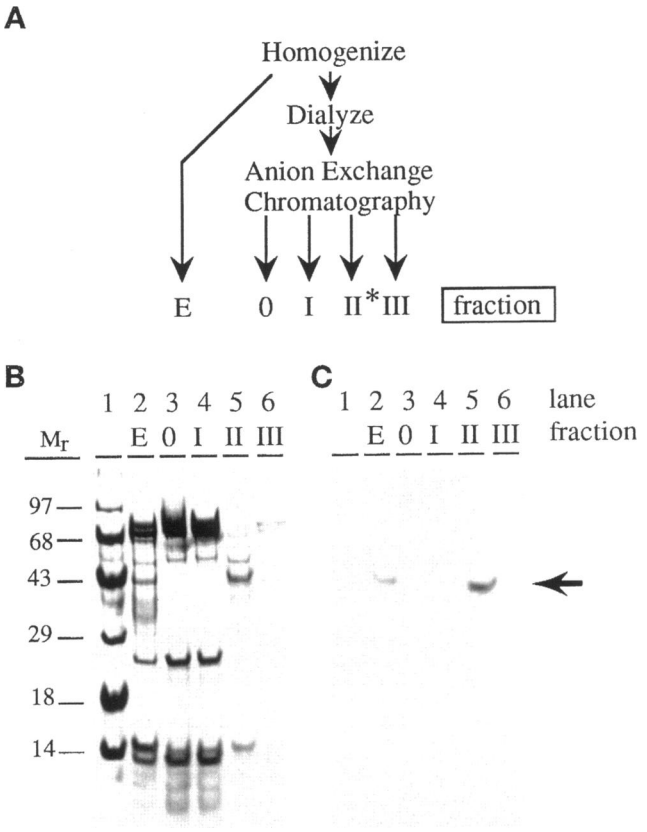

Figure 3. Partial purification of SPARC from the chicken CAM. (A) Proteins soluble in NP-40 were isolated from day 10 CAMs and fractionated by anion-exchange chromatography (see MATERIALS AND METHODS). E, unfractionated extract; 0, unbound fraction; I, proteins eluted with 75 mM NaCl; II, proteins eluted with 175 mM NaCl; III, proteins eluted with 500 mM NaCl. *, indicates the elution position of chicken, murine, and human SPARC. (B and C) SDS-PAGE and immunoblot analyses of fractions described in panel A. (B) Amido black stain for visualization of total protein. (C) Immunoblot analysis with anti-$SPARC_{254-273}$ peptide IgG. Lane 1, molecular weight standards; lane 2, unfractionated extract (E); lane 3, fraction 0; lane 4, fraction I; lane 5, fraction II; lane 6, fraction III. Arrow in panel C indicates immunoreactive band of approximately 40 kDa. M_r indicates the position and molecular weight ($\times 10^{-3}$) of protein standards shown in lane 1, panel B.

growth of the CAM (Figure 5A). Northern analysis of SPARC mRNA revealed two predominant transcripts (2.2 kb and 1.8 kb), as previously observed in chicken tissues (Bassuk *et al.*, 1993). Figure 6 illustrates the levels of SPARC protein, the 35-kDa SPARC degradation product, and SPARC mRNA during development of the CAM. The production of SPARC mRNA was highest during those intervals over which the levels of degraded SPARC protein were maximal. Since maximal mRNA levels were observed during days 10–13, the capacity for SPARC synthesis remained high during periods over which the protein appeared to be undergoing proteolysis. The mRNA profile was identical in four independent RNA isolations. Steady-state mRNA levels were consistent with the possibility that the decrease in SPARC protein after day 7 was the result of proteolytic cleavage.

Because of the increased vascularity of the CAM, we were concerned about the possible contribution of SPARC from chicken plasma or from cellular elements of the blood, such as thrombocytes, the avian equivalent of platelets. SPARC has been identified in human platelet α-granules and in human serum at 200 ng/ml (Malaval *et al.*, 1987). Therefore, we isolated protein and mRNA from the blood of chicken embryos at days 5, 7, 10, 14, and 17. Neither SPARC protein nor mRNA was detected by immunoblot or Northern analysis, respectively (unpublished experiments). These results indicated that the SPARC protein detected in our extracts was not derived from blood; therefore, the source of SPARC was most likely the resident populations of cells in the CAM. These observations confirmed our previous immunohistochemical studies that identified SPARC in endothelial cells of the CAM, but not in blood (Figures 1 and 2) .

SPARC Is Degraded by Extracellular Proteases during Angiogenesis

The antibody used for analysis of chicken SPARC was directed against a C-terminal epitope, that is itself labile to proteolysis; therefore, so immunoblots would be unlikely to reveal breakdown products from the central region or the N-terminal region of the protein. To characterize further the proteolysis of SPARC, we tested the stability of exogenous [^{125}I]-SPARC protein after its application to CAM tissue. As illustrated in Figure 7A, the proteolytic capacity of CAM tissues increased progressively from day 9 through day 15. Three major products of 35 kDa, 14 kDa, and >10 kDa (dye front) were apparent (arrows). The highest levels of 35-kDa fragment were observed in extracts from day 11–13, with lesser amounts on day 9. Although the samples were adjusted to reflect equal cpm, almost no intact SPARC was detected in the extracts from day 13 (Figure 7A, lane 8). We assume that smaller degradation products, which were not retained in the fixed SDS-PAGE gels, accounted for the total radioactivity measured in the samples before electrophoresis. No degradation was observed after incubation of SPARC on CAMs of day 17 (Figure 7A, lane 11). Bovine serum albumin, which was added as a carrier protein in some experiments, was not degraded by the CAMs in these experiments (unpublished experiments). Addition of proteinase inhibitors blocked cleavage of iodinated SPARC in all the CAMs tested (Figure 7A, lanes 4, 6, 8, and 10). That proteolysis of exogenously supplied SPARC occurred up to day 15 was consistent with the conclusion that the decrease in the levels of endoge-

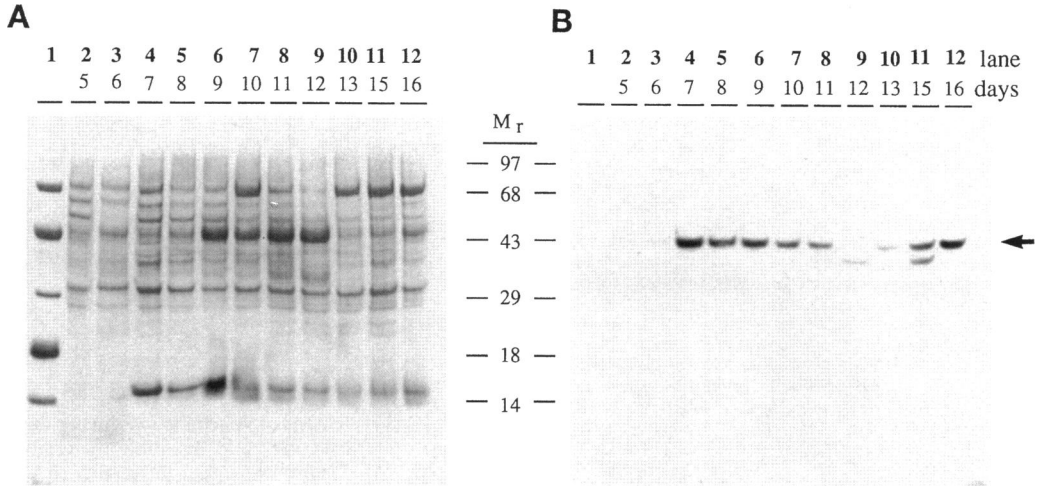

Figure 4. Biosynthesis of SPARC during development of the chicken CAM. Proteins soluble in NP-40 were isolated from staged CAMs and were fractionated by anion-exchange chromatography. Fractions that contained SPARC (fraction II) were resolved by SDS-PAGE and were transferred to a nitrocellulose membrane. An equal amount of protein was loaded in each lane. (A) Total protein visualized by staining of transferred proteins with amido black. (B) Immunodetection of SPARC on the same blot with an anti-SPARC$_{254-273}$ peptide antibody. The antibody reacted with a protein of approximately 40 kDa (arrow) that was differentially expressed during CAM development. A second band of approximately 35 kDa was also detected (days 11–15). M_r indicates the position and molecular weight ($\times 10^{-3}$) of standards shown in lane 1, panels A and B. "days", indicates developmental age.

nous SPARC shown in Figure 4 was the result of endogenous proteolytic activity.

The pattern of cleavage observed in Figure 7A appeared similar to the profile described previously for SPARC after digestion with plasmin, i.e., major products of 35 kDa/30 kDa and 14 kDa (Sage *et al.*, 1984). Experiments were therefore conducted to determine whether the degradation of SPARC by CAM tissue was similar to that produced by plasmin. Figure 7B shows immunoblots with three antisera that recognize distinct epitopes on human SPARC. The fragments generated after digestion of human SPARC by plasmin and by a day 15 CAM exhibited similar M_r on both anti-SPARC and anti-4.2 immunoblots (Figure 7B, lanes 2 and 4). In addition, the anti-2.3 antibody identified a 29-kDa

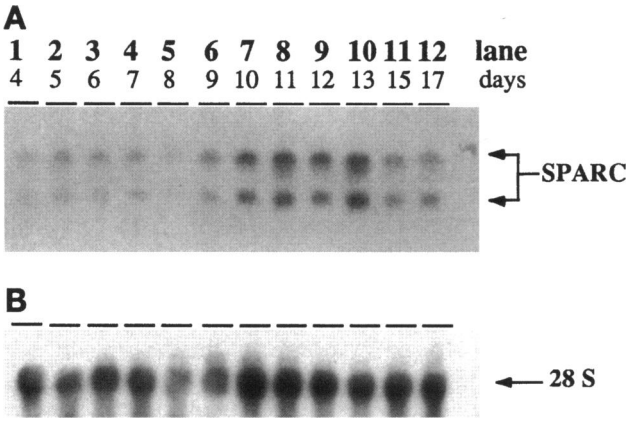

Figure 5. Steady-state levels of SPARC mRNA during development of the CAM. Total RNA was isolated from CAMs at embryonic days 4–17. (A) Samples were subjected to electrophoresis under denaturing conditions, transferred to nitrocellulose, and hybridized with a chicken SPARC cDNA probe. Two transcripts of 2.2 and 1.8 kb were apparent (arrows). (B) A 28 S rRNA cDNA probe was used to normalize for loading and transfer of samples after quantification of signal.

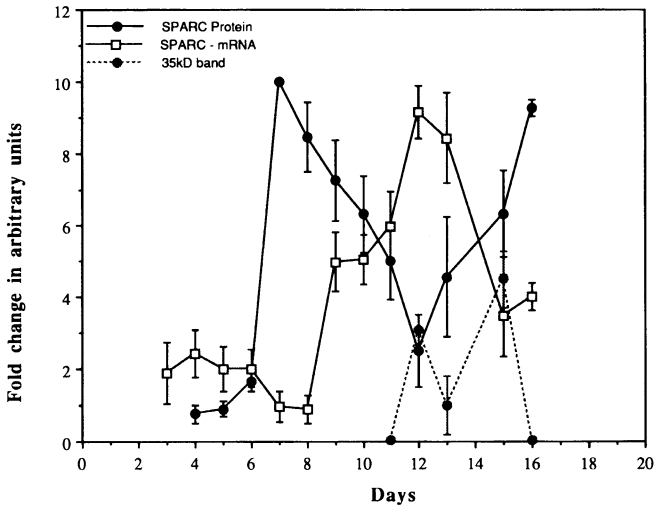

Figure 6. Profile of SPARC protein and mRNA during CAM development. Levels of SPARC protein were assessed by scanning densitometry of immunoblots from three independent experiments. mRNA levels from four independent experiments were determined by a phosphor image analyzer and were normalized to the 28 S signal to correct for loading and transfer efficiency. For comparison of both protein and mRNA, maximum values in both cases were normalized to 10 and all other values were adjusted accordingly. The 35-kDa cleavage product was also scanned and has been included in this profile. Points represent the mean ± SE.

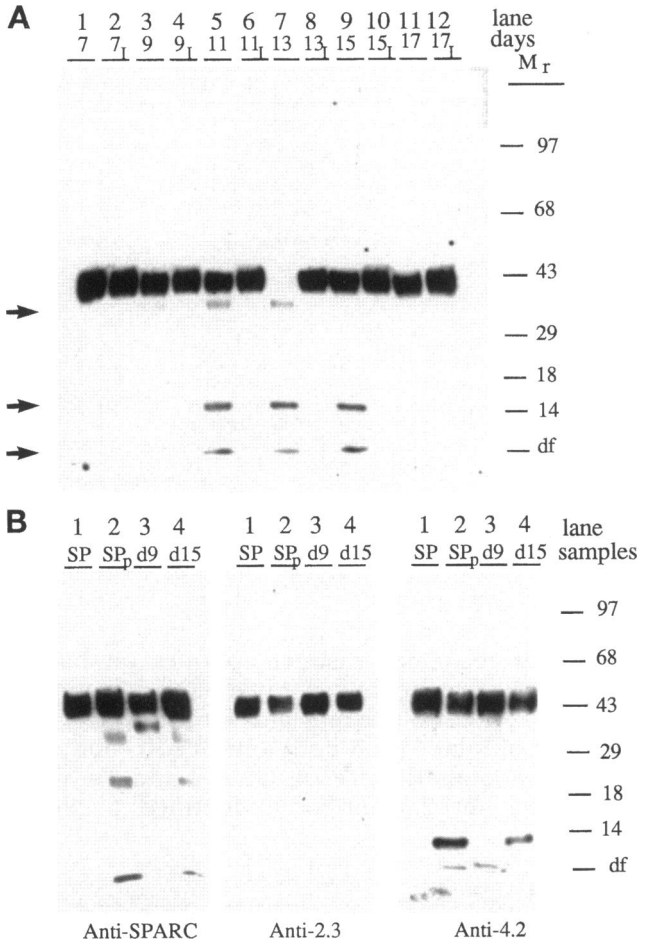

Figure 7. SPARC is degraded by extracellular proteases of the CAM. (A) 0.5 ng of [^{125}I]-SPARC was placed on staged CAMs at 37°C for 9 h in the presence or absence of proteinase inhibitors (I). After incubation, the area containing SPARC was dissected and homogenized in the presence of proteinase inhibitors. Samples containing equal counts were subjected to SDS-PAGE followed by autoradiography. Lanes 1 and 2, day 7 CAM; lanes 3 and 4, day 9 CAM; lanes 5 and 6, day 11 CAM; lanes 7 and 8, day 13 CAM; lanes 9 and 10, day 15 CAM; lanes 11 and 12, day 17 CAM. Arrows identify degradation products of 35 kDa, 14 kDa, and those in the dye front (>10 kDa). (B) SPARC immunoblots. SPARC (lane 1), SPARC incubated with plasmin (lane 2), SPARC incubated on a day 9 CAM (lane 3), and SPARC incubated on a day 15 CAM (lane 4). Antibodies are indicated below each blot: Anti-SPARC; anti-2.3, anti-SPARC$_{113-130}$ peptide; anti-4.2, anti-SPARC$_{254-273}$ peptide IgG.

product after incubation with a day 15 CAM that was not apparent in the plasmin digest. This fragment of SPARC was likely produced by additional protease or proteases in these tissues.

To verify that plasmin was present in these extracts, we determined the levels of active plasmin during CAM development (Table 2). Although plasmin activity was apparent throughout development, a correlation was observed between the peak of this enzyme at days 7–15 and maximal degradation of SPARC protein. Plasmin thus appears to be a candidate enzyme for the proteolysis of SPARC in vivo.

Table 2. Levels of plasmin during CAM development

Day[a]	Concentration[b]
5	1.3 μg/ml (±0.3)
6	1.4 μg/ml (±0.09)
7	1.86 μg/ml (±0.2)
8	1.8 μg/ml (±0.3)
9	1.8 μg/ml (±0.2)
10	1.6 μg/ml (±0.08)
11	2.1 μg/ml (±0.2)
13	1.8 μg/ml (±0.1)
15	1.8 μg/ml (±0.05)
17	1.5 μg/ml (±0.1)
19	1.3 μg/ml (±0.2)

[a]CAMs at specific days during development were homogenized in cold PBS, and insoluble material was removed by centrifugation. Total protein concentration was assessed in each sample by a BCA Protein Assay Reagent (Pierce). Plasmin concentration was determined after incubation of equal amounts of protein extract with the chromogenic substrate S-2304.

[b]Units of absorbance were compared to a standard curve for plasmin that was generated simultaneously with each experiment. Values represent the mean (±SE) of three independent experiments.

A limitation of the plasmin assays was the lack of information on the distribution of the enzyme within the CAM. We therefore used an overlay assay to localize the expression of PAs in this tissue. The assay is dependent on the conversion of plasminogen into active plasmin by PAs. The plasminogen is supplied in agar that is overlaid directly onto the CAM; the overlay contains casein as a substrate for plasmin. After 8 h of incubation, distinct zones of caseinolysis were observed (Figure 8). Areas of lysis, indicative of PA activity, were largely concentrated in the periphery of the CAM in areas corresponding to region III. Activity was occasionally associated with large blood vessels and with areas of branching throughout the CAM. At later stages of development (after day 13), the degree of total lysis decreased significantly, and lytic foci were more discrete and observed largely near the periphery (region III) of the CAM (Figure 8, B and C). Essentially no PA activity was detected after day 16 (data not shown). Lytic activity was absent from controls, which included zymography in the presence of several inhibitors such as amiloride or in the absence of plasminogen (Figure 8E). These results indicate that plasmin is present in the CAM and that the activation of plasminogen by PAs occurs in areas in which expression of SPARC is enhanced.

Peptide Sequences of SPARC Are Angiogenic

Previous studies have shown that specific peptides derived from SPARC increased the number of cords in

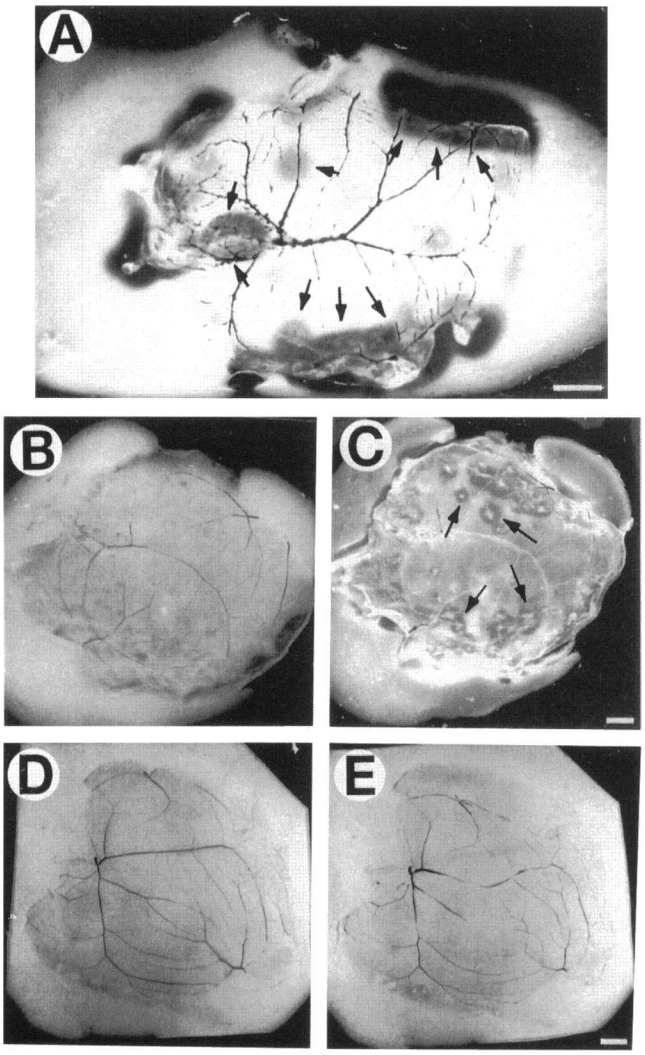

Figure 8. Distribution of plasminogen activator activity in the CAM. CAMs were dissected, placed onto a sterile glass surface, and overlaid with a suspension of agarose, casein, and plasminogen. The samples were incubated for 8 h at 37°C and were subsequently photographed under dark illumination. Areas of casein degradation appear more transparent i.e., as darker regions within the opaque gel (arrows). (A) day 10; (B and C) day 13; (D and E) day 14. For comparison, the preparations were photographed before (B and D) and after incubation (C and E). In D and E, the overlay lacked plasminogen. Relative transparency is not comparable between embryos due to differences in tissue transparency that occur with increased embryonic age. Bars = 100 μm.

an assay of angiogenesis in vitro and promoted the directional growth of CAM vessels in a methylcellulose pellet assay (Lane *et al.*, 1994). We compared intact SPARC and several SPARC-derived peptides, in a newly developed assay that allows a quantitative assessment of angiogenesis. In such experiments, angiogenic substances are known to induce directional growth of new vessels, perpendicular to the CAM, into a gel of type I collagen (Nguyen *et al.*, 1994). The growth of blood vessels against gravity abrogates several artifacts typically observed in other assays of angiogenesis. Suspensions of vitrogen (type I collagen) containing SPARC peptides, intact SPARC, bFGF, or BSA were placed onto the CAM for 24 h. The meshes were subsequently sectioned (Figure 9), and quantification of vessels that invaded the mesh was obtained morphometrically with the OPTIMAS program. Results are shown in Table 3.

Table 3. Angiogenic potential of SPARC and SPARC peptides in CAM assays

Protein/Peptide[a]	Concentration[b]	Capillary Density[c]
1. SPARC (4)[d]	0.1 mM	5 (±3)
2. bFGF (3)	0.01 mM	96 (±21)
3. PBS (5)	—	3 (±3)
4. BSA (2)	0.1 mM	6 (±4)
5. 4–23 (2)	0.5 mM	11 (±5)
6. 54–73 (2)	0.5 mM	7 (±4)
7. 113–130 (1)	0.01 mM	22
8. 113–130 (1)	0.05 mM	54
9. 113–130 (3)	0.5 mM	36 (±12)
10. $113–130_{H121-R}$ (2)	0.5 mM	12 (±3)
11. $113–130_{K119-A}$ (2)	0.5 mM	25 (±4)
12. 119–122 (1)	0.01 mM	59
13. 119–122 (1)	0.05 mM	125
14. 119–122 (3)	0.5 mM	250 (±52)
15. 119–122 (1)	5 mM	275
16. 120–122 (1)	0.05 mM	59
17. 120–122 (2)	0.5 mM	73 (±15)

[a]Peptides and proteins were solubilized in sterile PBS.

[b]Concentrations of the peptides were obtained by amino acid analysis of stock solutions.

[c]Capillary density is defined as the number of capillaries per mm^2 and is representative of the total volume of the mesh used in the assay. An average of capillary density is provided in those cases in which two or more experiments were quantified (±SD).

[d]Number of independent experiments.

A significant influx of fibroblasts was seen in control meshes that contained either PBS alone or BSA; however, capillaries were rare (Figure 9B). Meshes containing intact SPARC, peptide $SPARC_{4–23}$, or $SPARC_{54–73}$ showed no significant increase in the number of capillaries in comparison to negative controls (BSA) (Figure 9C and Table 3). In contrast, $SPARC_{113–130}$ induced capillary growth (Figure 9D and Table 3), and the angiogenic response to this peptide was concentration dependent. Amino acid substitutions in $SPARC_{113–130}$ at amino acids 119 and 121 diminished its activity (Figure 9E and Table 3). The sequence KGHK ($SPARC_{119–122}$) was responsible for most of the angiogenic response (Figure 9H). The effect of KGHK was also dose dependent, as shown in Figure 10 and Table 3. Although KGHK was more active than $SPARC_{113–130}$ at all concentrations tested, the activity of KGHK appeared comparable to $SPARC_{113–130}$ at concentrations below 0.05

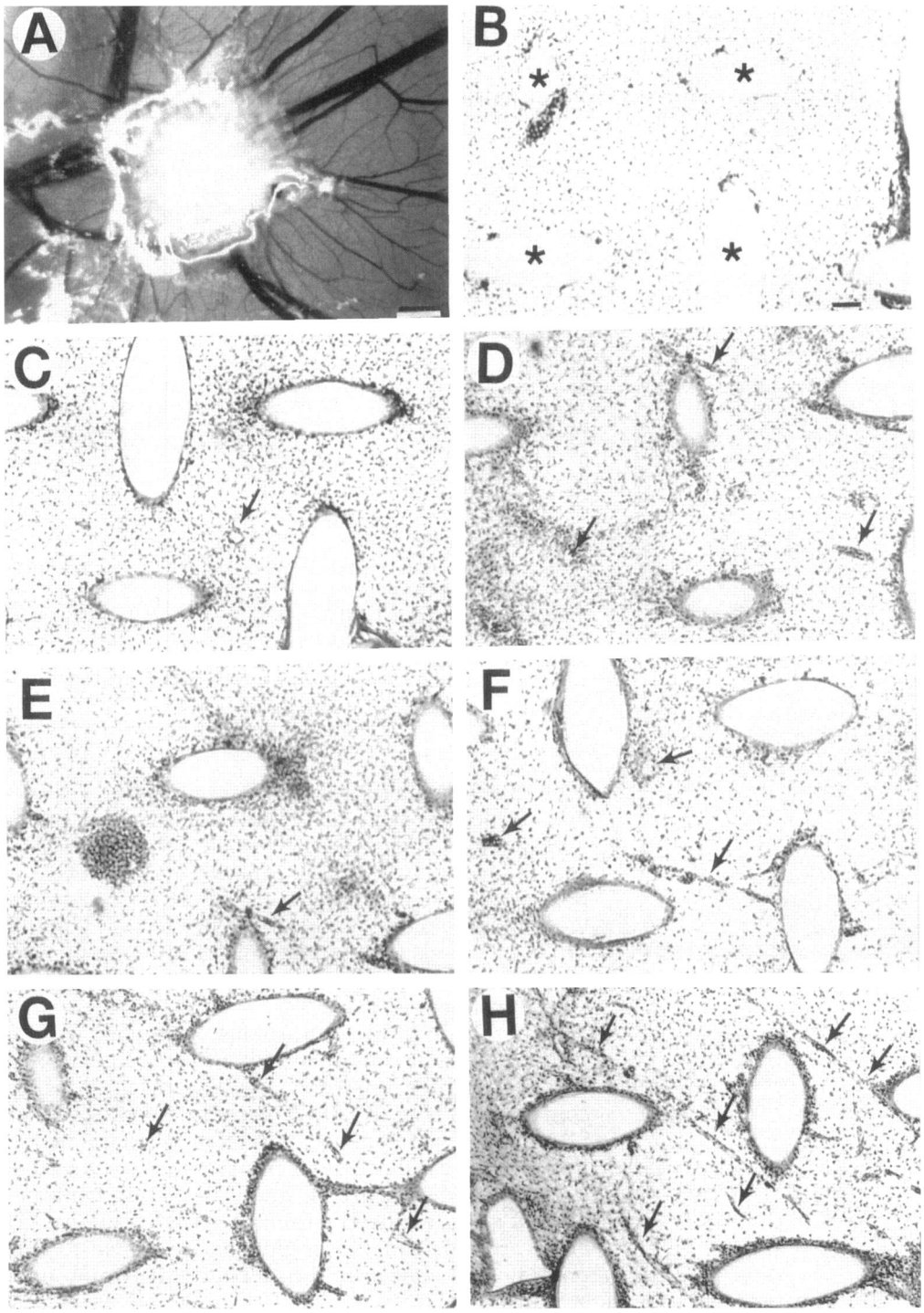

Figure 9. Effect of SPARC peptides on the invasion and proliferation of capillaries. Samples of vitrogen alone or vitrogen containing SPARC peptides were prepared as described in MATERIALS AND METHODS, cast into meshes, and applied onto CAMs. After 24 h, the preparations were removed, fixed, and sectioned. Identification of peptides and quantification of capillary density are shown in Tables 1 and 3, respectively. The asterisks in B depict transverse sections of the mesh structure. (A) A vitrogen gel between two meshes placed on a CAM; (B-H) photomicrographs of meshes that have been sectioned (10 μm) and stained with hematoxylin and eosin; (B) PBS; (C) $SPARC_{4-23}$; (D) $SPARC_{113-130}$; (E) $SPARC_{113-130K121-R}$; (F) GHK; (G) bFGF; (H) KGHK. Bars: A = 500 μm, B = 100 μm.

mM. Higher concentrations of $SPARC_{113-130}$ were less stimulatory, possibly because of solubility problems at the higher concentrations. Substitution of His_{121} with Arg markedly reduced the activity of KGHK, whereas substitution of Lys_{119} with Ala had little effect (Table 3). A slightly shorter peptide, GHK, was less effective than KGHK. In summary, much of the angiogenic activity of $SPARC_{113-130}$ was attributed to the sequence KGHK (aa 119–122), a peptide previously shown to bind copper and to be released after treatment of SPARC with plasmin (Lane *et al.*, 1994).

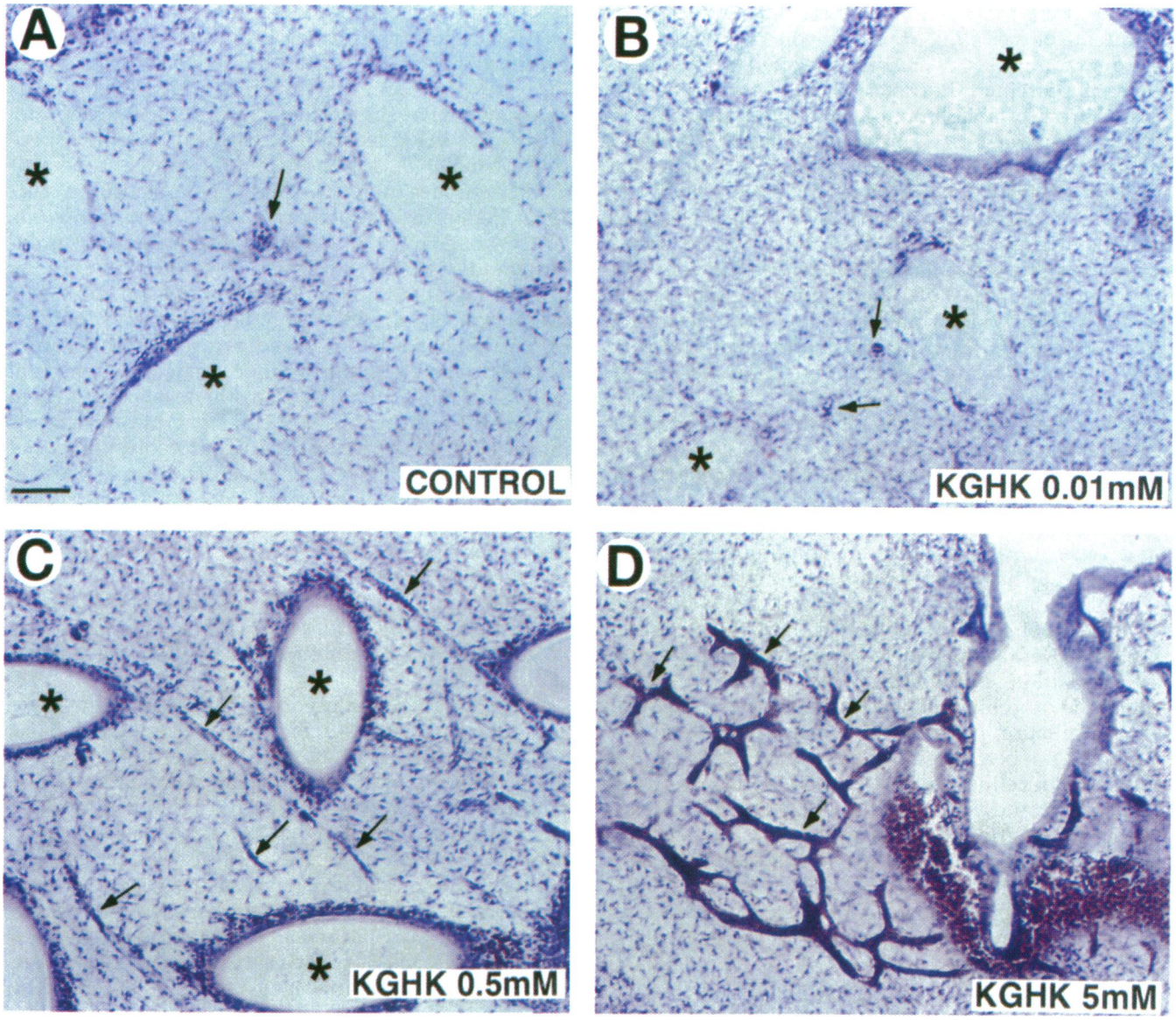

Figure 10. Concentration dependency of KGHK in capillary invasion. Vitrogen was cast with different concentrations of KGHK as indicated. Transverse sections of the mesh were stained with hematoxylin and eosin. Blood vessels are indicated by arrows. (A) Vitrogen and PBS; (B) KGHK, 0.01 mM; (C) KGHK, 0.5 mM; (D) KGHK, 5 mM. Asterisks depict openings in the nylon mesh. Bar = 100 μm.

DISCUSSION

SPARC is one of the major secretory products of endothelial cells in vitro (Sage *et al.*, 1984) and has been shown to bind to endothelial plasma membranes with high affinity (Yost and Sage, 1993). Several characteristics of SPARC expression have implicated a role for this protein in the regulation of tissue growth and remodeling (Sage *et al.*, 1989*b*; Iruela-Arispe *et al.*, 1991a,b; Reed *et al.*, 1993; Lane *et al.*, 1994). In this study, we provide evidence that SPARC is directly associated with blood vessel formation in vivo, and have identified a novel posttranslational mechanism involved in the regulation of SPARC during this process. Our results indicate that SPARC is expressed by endothelial cells and demonstrate that the protein is a substrate for plasmin, a protease implicated in the formation of new capillaries.

SPARC mRNA and protein were detectable in the CAM by day 5 of normal embryonic development. The 10-fold increase in SPARC protein by day 7 appeared to correlate with maximal rates of CAM expansion that were maintained through day 12 of embryonic growth. In contrast, induction of SPARC mRNA appeared to lag behind protein expression by almost

24 h. Several interpretations of these data are possible: 1) Protein synthesis might remain constant while protein degradation is decreased; elevated steady-state levels of protein thus occur. 2) New protein is expressed from a labile pool of mRNA not detected in total CAM extracts. 3) There is considerable ability to increase expression of SPARC protein in the absence of increased levels of mRNA. This last possibility is supported by studies in vitro. SPARC protein has been shown to increase in the absence of new RNA synthesis after exposure of cells to TGF-β (Wrana *et al.*, 1991) or heat shock (Sauk *et al.*, 1991). Therefore, the induction of SPARC protein might occur in response to a rapid change in SPARC translation from existing RNA, or as a result of increased transcription of SPARC mRNA.

We have also described the regulated degradation of SPARC protein during periods of peak synthesis in vivo. Recently, we demonstrated that proteolysis of SPARC in solution resulted in the release of peptides that were potent stimulators of endothelial cell growth (Lane *et al.*, 1994), an interesting finding because the intact protein has been shown to inhibit endothelial cell proliferation (Funk and Sage, 1991, 1993). Because the function of several growth factors is controlled by proteases (Neurath, 1989; Lyons *et al.*, 1990; Flaumenhaft and Rifkin, 1991, 1992), it was conceivable that proteolytic processing of SPARC might also contribute to the regulation of its activity. Indeed, extracellular enzymes have been shown to promote the processing of many extracellular matrix proteins (Neurath, 1989; Flaumenhaft and Rifkin, 1991, 1992) and to activate and inactivate growth factors such as TGF-β and IL-1 (Sato and Rifkin, 1989; Lyons *et al.*, 1990; Sleath *et al.*, 1990). Rapid proteolysis of SPARC would also be consistent with a regulatory role for the intact protein at sites of morphogenesis and repair (Holland *et al.*, 1987; Sage *et al.*, 1989a; Reed *et al.*, 1993).

Although SPARC is a secreted protein, its half life in the extracellular space appears to be short. Most immunocytochemical analyses have revealed intracellular distributions in tissues that nevertheless exhibit high levels of expression. Extracellular SPARC is detected predominantly in newly formed bone matrix and in Reichert's membrane, areas abundant in types I and IV collagen, respectively. Indeed, SPARC binds to both collagens (Termine, 1981; Sage *et al.*, 1989b; Mayer *et al.*, 1991), a property that could account for its extracellular accumulation. Because SPARC is rarely detected in the extracellular space, it is likely that rapid turnover or clearance occurs after secretion. In vitro, SPARC has been shown to be susceptible to cleavage by a number of extracellular proteases that include cathepsins, stromelysin, neutral metalloproteases, elastase, and serine proteases such as trypsin and plasmin (Sage *et al.*, 1984; Tyree, 1989; Maurer *et al.*, 1992; Page *et al.*, 1993; Lane *et al.*, 1994). Nevertheless, the physiological degradation of SPARC in vivo has not been investigated. Our experiments provide evidence that SPARC is rapidly cleaved after secretion in tissues displaying active angiogenesis. In a previous study, we have shown that plasmin-mediated proteolysis of SPARC led to the release of bioactive peptides (Lane *et al.*, 1994). Plasmin is known to be activated in tissues undergoing angiogenesis (Rifkin *et al.*, 1982; Pepper and Montesano, 1990; Bacharach *et al.*, 1992). Moreover, the activation of plasmin by urokinase and tissue-type PAs is regulated by several growth factors that stimulate blood vessel formation (Montesano *et al.*, 1986, 1990). Because the production of plasmin has been proposed as a controlling feature of blood vessel growth, we investigated the temporal activation of plasmin as well as the location of PAs in the CAM. Our results indicate that plasmin levels increase during periods of SPARC proteolysis and that PAs are localized to regions of active vascular growth, a distribution similar to that of SPARC. Definitive proof that plasmin is one of the enzymes involved in the proteolysis of SPARC in vivo is currently lacking. However, plasmin is known to play a central role in the activation of additional enzymes implicated in tissue remodeling (He *et al.*, 1989), one of which, stromelysin, has been shown to degrade SPARC (Lane *et al.*, 1994).

In the past we have used synthetic peptides to identify potential activities of SPARC (Lane and Sage, 1990; Lane *et al.*, 1992; Funk and Sage, 1991, 1993). In many cases, peptides were able to mimic and/or compete functionally with the native protein (Lane and Sage, 1990; Yost and Sage, 1993). In other cases, however, the physiological relevance of their activity has been difficult to establish, because these regions do not appear to be exposed in the intact protein. This reservation applies in particular to domain II of SPARC (amino acids 53–130), a region composed of two cationic sequences that appear to have opposite effects on the proliferation of endothelial cells. Peptides from the first cationic region (amino acids 54–73) mimic the inhibition of proliferation mediated by the intact protein on endothelial cells and fibroblasts (Funk and Sage, 1991, 1993). In contrast, significantly lower concentrations of peptides from the second cationic region (amino acids 113–130) stimulate proliferation of the same cells (Funk and Sage, 1993; Lane *et al.*, 1994). Recently, experiments with peptides from domain IV (amino acids 254–273) have demonstrated a synergistic effect in combination with a SPARC sequence from domain II (amino acids 54–73) on the inhibition of cell cycle progression (Sage *et al.*, 1994). Domain IV is normally exposed in the protein and binds to cell-surface receptors (Yost and Sage, 1993). It is most likely that the inhibition of the cell cycle mediated by SPARC occurs as a result of a synergistic interaction between these two regions.

The proliferative activity of the second cationic fragment of domain II was somewhat unexpected, because intact SPARC exhibited an inhibitory effect on the cell cycle (Funk and Sage, 1993). Evidence that peptides from this region could be released after incubation with plasmin or trypsin (Lane *et al.*, 1994) provided a novel interpretation of these results, i.e., this sequence might be unmasked after proteolytic processing. Since there was evidence for proteolytic processing in the CAM, we reassessed the angiogenic capacity of SPARC and SPARC-derived peptides in a newly developed quantitative assay of angiogenesis (Nguyen *et al.*, 1994). Both KGHK and a larger peptide from domain II that contains this sequence displayed significant angiogenic activity and thus corroborate previous data (Lane *et al.*, 1994). Because SPARC itself was inactive in the assay, we concluded that proteolysis was necessary to expose angiogenic sequences. However, intact SPARC has previously been shown to stimulate cord formation in cultured endothelial cells, an assay thought to mimic some aspects of angiogenesis (Lane *et al.*, 1994). A possible complication of these angiogenesis assays in the CAM is the use of substrates, such as collagen, that bind SPARC and thereby prevent access to endothelial cells. For this reason, we are unable to make further statements concerning the angiogenic potential of native SPARC in vivo.

Plasmin can also release GHK from SPARC (Lane *et al.*, 1994); the effects of this peptide were similar, although not as pronounced as those of KGHK. GHK, also known as liver cell growth factor, has been studied for several years (Raju *et al.*, 1982; Pickart, 1983; Pickart and Lovejoy, 1987; Maquart *et al.*, 1993). It was originally isolated from human plasma and was claimed to stimulate angiogenesis (Pickart and Lovejoy, 1987) and accelerate wound repair (Maquart *et al.*, 1993). We have proposed that SPARC is a source of this peptide (Lane *et al.*, 1994).

The specific mechanism by which KGHK/GHK enhances angiogenesis remains unclear, although our previous studies would imply a direct stimulation of proliferation (Funk and Sage, 1993). Both KGHK and GHK have been shown to bind copper with high affinity (Pickart and Lovejoy, 1987; Lane *et al.*, 1994), and copper availability has been correlated with angiogenesis. For example, copper increases systemically during inflammation and focally in areas of neovascularization (Ziche *et al.*, 1982; Apelgot *et al.*, 1986). Copper also influences the synthesis of several extracellular matrix proteins, such as collagen and fibronectin (Hannan and McAuslan, 1982; Maquart *et al.*, 1993), the expression of which appears to be enhanced during angiogenesis (Risau and Lemmon, 1989). Finally, copper-deficient animals are compromised in their response to angiogenic factors and have a diminished ability to vascularize tumors (Ziche *et al.*, 1982; Brem *et al.*, 1990). Although it is conceivable that copper mediates one or more aspects of the angiogenic response, it is important to emphasize that copper alone does not appear to have the same effect as either KGHK or GHK. Copper itself is not sufficient to promote an angiogenic response (Raju *et al.*, 1982; Lane *et al.*, 1994) or to accelerate wound healing (Maquart *et al.*, 1993). Molecular signals resulting from the exposure of cells to KGHK/GHK are at this point unknown.

The data presented in this study support several conclusions: 1) SPARC is expressed transiently by endothelial cells involved in angiogenesis. The level of SPARC expression is higher in small capillaries than in large and developmentally older vessels. 2) SPARC is degraded in the extracellular matrix during periods of rapid vascular morphogenesis. 3) Plasmin is found near sites of SPARC expression in the CAM. This protease mimics the fragmentation pattern of SPARC produced by the CAM. Plasmin might contribute to the activation of other proteases that also degrade SPARC. 4) Intact SPARC does not appear to mediate an angiogenic response. 5) Regions of SPARC between amino acids 119–122 are angiogenic and are likely released during proteolytic cleavage of the protein. Collectively, the observations indicate a dual role for SPARC as a regulator of cell proliferation. A combination of negative and positive effects on endothelial cell proliferation can be envisioned that is dependent upon the availability of proteases and/or stabilizing effects of the matrix. At sites where proliferation is required, degradation of extracellular SPARC might promote the release of bioactive peptides that stimulate angiogenesis. In the absence of specific proteolysis, the protein remains intact, acts negatively on cell cycle progression, and disrupts cell-matrix interactions, activities thought to facilitate migration and tissue remodeling (Sage *et al.*, 1989b).

ACKNOWLEDGMENTS

Funding for this study was provided by American Heart Association grant 93–1197 and National Institutes of Health grants GM-40711 and HL-03174. T.F.L. was supported by a National Institutes of Health Predoctoral training grant HL-07312.

REFERENCES

Apelgot, S., Coppey, J., Fromentin, A., Guille, E., Poupoon, M.F., and Roussel, A. (1986). Altered distribution of copper (64 Cu) in tumor bearing mice and rats. Anticancer Res. *6*, 159–164.

Auerbach, R., Kubai, L., Knighton, D., and Folkman, J. (1974). A simple procedure for the long-term cultivation of chicken embryos. Dev. Biol. *41*, 391–394.

Ausprunk, D.H., Knighton, D.R., and Folkman, J. (1974). Differentiation of vascular endothelium in the chicken chorioallantois: a structural and autoradiographic study. Dev. Biol. *38*, 237–249.

Bacharach, E., Itin, A., and Keshet, E. (1992). In vivo patterns of expression of urokinase and its inhibitor PAI-1 suggest a concerted role in regulating physiological angiogenesis. Proc. Natl. Acad. Sci. USA *89*, 10686–10690.

Bassuk, J., Iruela-Arispe, M.L., Lane, T.F., Benson, J., Berg, R.A., and Sage, E.H. (1993). Molecular analysis of chicken embryo SPARC. Eur. J. Biochem. *218*, 117–127.

Bolender, R.P. (1993). Software for quantitative immunogold and in situ hybridization. Microsc. Res. Tech. *25*, 304–313.

Bolender, R.P., and Charleston, J.S. (1993). Software for counting cells and estimating structural volumes with the optical disector and fractionator. Microsc. Res. Tech. *25*, 314–324.

Brændgaard, H., Evans, S.M., Howard, C.V., and Gundersen, H.J.G. (1990). The total number of neurons in the human neurocortex unbiasedly estimated using optical dissectors. J. Microsc. *159*, 285–304.

Brem, S.S., Zagzag, D., Tsanaclis, A.M., Gately, S., Elkouby, M.P., and Brien, S.E. (1990). Inhibition of angiogenesis and tumor growth in the brain: suppression of endothelial cell turnover by penicillamine and the depletion of copper, an angiogenic cofactor. Amer. J. Pathol. *137*, 1121–1142.

Clezardin, P., Malaval, L., Ehrensperger, A., Delmas, P.D., Dechavanne, M., and McGregor, J.L. (1988). Complex formation of human thrombospondin with osteonectin. Eur. J. Biochem. *175*, 275–284.

Flaumenhaft, R., and Rifkin, D.B. (1991). Extracellular matrix regulation of growth factor and protease activity. Curr. Opin. Cell Biol. *3*, 817–823.

Flaumenhaft, R., and Rifkin, D.B. (1992). The extracellular regulation of growth factor action. Mol. Biol. Cell *3*, 1057–1065.

Folkman, J., and Klagsbrun, M. (1987). Angiogenic factors. Science *235*, 345–349.

Funk, S.E., and Sage, E.H. (1991). The Ca^{2+}-binding glycoprotein SPARC modulates cell cycle progression in bovine aortic endothelial cells. Proc. Natl. Acad. Sci. USA *88*, 2648–2652.

Funk, S.E., and Sage, E.H. (1993). Differential effects of SPARC and cationic SPARC peptides on DNA synthesis by endothelial cells and fibroblasts. J. Cell Physiol. *154*, 53–63.

Gundersen, H.J.G. (1986). Stereology of arbitrary particles: a review of unbiased number and size estimators and the presentation of some new ones. J. Microsc. *143*, 3–45.

Gundersen, H.J.G., Bagger, P., Bendtsen, T.F., Evans, S.M., Korbo, L., Marcussen, N., Møller, A., Nielsen, K., Nyengaard, J.R., Pakkenberg, B., Sorensen, F.B., Vesterby, A., and West, M.J. (1988). The new stereological tools: disector, fractionator and point sampled intercepts and their use in pathological research and diagnosis. Acta Pathol. Microbiol. Immunol. Scand. *96*, 857–881.

Gundersen, H.J.G., and Jensen, E.B. (1987). The efficiency of systematic sampling in stereology and its prediction. J. Microsc. *147*, 229–263.

Hannan, G.N., and McAuslan, B.R. (1982). Modulation of synthesis of specific proteins in endothelial cells by copper, cadmium, and disulfiram: an early response to an angiogenic inducer of cell migration. J. Cell. Physiol. *111*, 207–212.

He, C., Wilhelm, S.M., Pentland, A.P., Marmer, B.L., Grant, G.A., Eisen, A.Z., and Goldberg, G.I. (1989). Tissue cooperation in a proteolytic cascade activating human interstitial collagenase. Proc. Natl. Acad. Sci. USA *86*, 2632–2636.

Holland, P.W.H., Harper, S.J., McVey, J.H., and Hogan, B.L.M. (1987). In vivo expression of mRNA for the Ca^{++}-binding protein SPARC (osteonectin) revealed by in situ hybridization. J. Cell. Biol. *105*, 473–482.

Iruela-Arispe, M.L., Diglio, C., and Sage, H. (1991a). Modulation of extracellular matrix proteins by endothelial cells undergoing angiogenesis in vitro. Arterioscler. Thromb. *11*, 805–815.

Iruela-Arispe, M.L., Hasselaar, P., and Sage, E.H. (1991b). Differential expression of extracellular proteins is correlated with angiogenesis in vitro. Lab. Invest. *64*, 174–186.

Iruela-Arispe, M.L., Liska, D.A., Sage, E.H., and Bornstein, P. (1993). Differential expression of thrombospondin 1, 2, and 3 during murine development. Dev. Dynamics *197*, 40–56.

Laemmli, U.K. (1970). Cleavage of structural proteins during the assembly of the head of bacteriophage T4. Nature *277*, 680–685.

Lane, T.F., Iruela-Arispe, M.L., Johnson, R., and Sage, E.H. (1994). SPARC is a source of copper-binding peptides that stimulate angiogenesis. J. Cell Biol. *125*, 928–937.

Lane, T.F., Iruela-Arispe, M.L., and Sage, E.H. (1992). Regulation of gene expression by SPARC during angiogenesis in vitro: changes in fibronectin, thrombospondin-1, and plasminogen activator inhibitor-1. J. Biol. Chem. *267*, 16736–16745.

Lane, T.F., and Sage, E.H. (1990). Functional mapping of SPARC: peptides from two distinct sites modulate cell adhesion. J. Cell. Biol. *111*, 3065–3076.

Lane, T.F., and Sage, E.H. (1994). The biology of SPARC: a protein that modulates cell-matrix interactions. FASEB J. *8*, 163–173.

Lyons, R.M., Gentry, L.E., Purchio, A.F., and Moses, H.L. (1990). Mechanism of activation of latent recombinant transforming growth factor β1 by plasmin. J.Cell Biol. *110*, 1361–1367.

Malaval, L., Fournier, B., and Delmas, P.D. (1987). Radioimmunoassay for osteonectin: concentrations in bone, nonmineralized tissues, and blood. J. Bone Miner. Res. *2*, 457–465.

Maquart, F.X., Bellon, G., Chaquor, C., Wegrowski, J., Patt, L.M., Trachy, R.E., Monboisse, J.C., Chastang, F., Birembaut, P., Gillery, P., and Borel, J.P. (1993). In vivo stimulation of connective tissue accumulation by the tripeptide-copper complex glycyl-L-histidyl-L-lysine-Cu^{2+} in rat experimental wounds. J. Clin. Invest. *92*, 2368–2376.

Mason, I.J., Taylor, A., Williams, J.G., Sage, H., and Hogan, B.L.M. (1986). Evidence from molecular cloning that SPARC, a major product of mouse embryo parietal endoderm, is related to an endothelial cell "culture shock" glycoprotein. EMBO J. *5*, 1465–1472.

Maurer, I.J., Mayer, U., Bruch, M., Mann, K., Landwehr, R., Engel, J., and Timpl, R. (1992). High-affinity and low-affinity calcium binding and stability of the multidomain extracellular 40 kDa basement membrane glycoprotein (BM-40/SPARC/osteonectin). Eur. J. Biochem. *204*, 233–240.

Mayer, U., Aumailley, M., Mann, K., Timpl, R., and Engel, J. (1991). Calcium-dependent binding of basement membrane protein BM-40 (osteonectin, SPARC) to basement membrane collagen type IV. Eur. J. Biochem. *198*, 141–150.

Montesano, R., Pepper, M., and Orci, L. (1990). Angiogenesis in vitro: morphogenetic and invasive properties of endothelial cells. News Physiol. Sci. *5*, 75–79.

Montesano, R., Vassalli, J.D., Baird, A., Guillemin, A., and Orci, L. (1986). Basic fibroblast growth factor induces angiogenesis in vitro. Proc. Natl. Acad. Sci. USA. *83*, 7297–7301.

Neurath, H. (1989). Proteolytic processing and physiological regulation. Trends Biochem. Sci. *14*, 268–271.

Nguyen, M., Shing, Y., and Folkman, J. (1994). Quantitation of angiogenesis and antiangiogenesis in the chick embryo choriallantoic membrane. Microvasc. Res. *47*, 31–40.

Otsuka, K., Yao, K.L., Wasi, S., Tung, P.S., Aubin, J.E., Sodek, J., and Termine, J.D. (1984). Biosynthesis of osteonectin by fetal porcine calvarial cells in vitro. J. Biol. Chem. *259*, 9805–9812.

Page, A.E., Hayman, A.R., Andersson, L.M.B., Chambers, T.J., and Warburton, M.J. (1993). Degradation of bone matrix proteins by osteoclast cathepsins. Int. J. Biochem. *25*, 545–550.

Pepper, M.S., and Montesano, R. (1990). Proteolytic balance and capillary morphogenesis. Cell. Differ. Dev. *32*, 319–327.

Pickart, L. (1983). The biological effects and mechanism of action of the plasma tripeptide glycyl-L-histidyl-L-lysine. Lymphokines *8*, 425–446.

Pickart, L., and Lovejoy, S. (1987). Biological activity of human plasma copper-binding growth factor glycyl-L-histidyl-L-lysine. Methods Enzymol. *147*, 314–328.

Raines, E.W., Lane, T.F., Iruela-Arispe, M.L., Ross, R., and Sage, E.H. (1992). The extracellular glycoprotein SPARC interacts with platelet-derived growth factor (PDGF)-AB and BB and inhibits binding of PDGF to its receptor. Proc. Natl. Acad. Sci USA. *89*, 1281–1285.

Raju, K.S., Alessandri, G., Ziche, M., and Gullino, P.N. (1982). Ceruloplasmin, copper ions and angiogenesis. J. Natl. Cancer Inst. *69*, 81–88.

Reed, M.J., Puolakkainen, P., Lane, T.F., Dickerson, D., Bornstein, P., and Sage, E.H. (1993). Differential expression of SPARC and thrombospondin 1 in wound repair: immunolocalization and in situ hybridization. J. Histochem. Cytochem. *41*, 1467–1477.

Rifkin, D.B., Gross, J.L., Moscatelli, D., and Jaffe, E. (1982). Proteases and angiogenesis: production of plasminogen activator and collagenase by endothelial cells. In: Pathobiology of the Endothelial Cell, ed., H.L. Nossel and H.J. Vogel, New York: Academic Press, 191–197.

Risau, W., and Lemmon, V. (1989). Changes in the vascular extracellular matrix during embryonic vasculogenesis and angiogenesis. Dev. Biol. *74*, 134–142.

Sage, E.H., Bassuk, J.A., Yost, J.C., Folkman, M.J., and Lane, T.L. (1995). Inhibition of endothelial cell proliferation by SPARC is mediated through a calcium-binding EF-hand sequence. J. Cell. Biochem. *57*, 127–140.

Sage, H., Johnson, C., and Bornstein, P. (1984). Characterization of a novel serum albumin-binding glycoprotein secreted by endothelial cells in culture. J. Biol. Chem. *259*, 3993–4007.

Sage, H., Vernon, R.B., Decker, J., Funk, S.E., and Iruela-Arispe, M.L. (1989a). Distribution of the calcium-binding protein SPARC in tissues of embryonic and adult mice. J. Histochem. Cytochem. *37*, 819–829.

Sage, H., Vernon, R.B., Funk, S.E., Everitt, E.A., and Angello, J. (1989b). SPARC, a secreted protein associated with cellular proliferation, inhibits cell spreading in vitro and exhibits Ca^{2+}-dependent binding to the extracellular matrix. J. Cell Biol. *109*, 341–356.

Sappino, A.P., Huarte, J., Vassalli, J.D., and Belin, D. (1991). Sites of synthesis of urokinase and tissue-type plasminogen activators in the murine kidney. J. Clin. Invest. *87*, 962–970.

Sato, Y., and Rifkin, D.B. (1989). Inhibition of endothelial cell movement by pericytes and smooth muscle cells: activation of latent transforming growth factor-beta 1-like molecule by plasmin during co-culture. J. Cell Biol. *109*, 309–315.

Sauk, J.J., Norris, K., Kerr, J.M., Somerman, M.J., and Young, M.F. (1991). Diverse forms of stress result in changes in cellular levels of osteonectin/SPARC without altering mRNA levels in osteoligament cells. Calcif. Tissue Int. *49*, 58–62.

Schägger, H., and von Jagow, G. (1987). Tricine-sodium dodecyl sulfate-polyacrylamide gel electrophoresis for the separation of proteins in the range from 1 to 100 kDa. Anal. Biochem. *166*, 368–379.

Sleath, P.R., Hendrickson, R.C., Kronheim, S.R., March, C.J., and Black, R.A. (1990). Substrate specificity of the protease that processes human interleukin-1β. J. Biol. Chem. *265*, 14526–14528.

Stenner, D.D., Tracy, R.P., Riggs, B.L., and Mann, K.G. (1986). Human platelets contain and secrete osteonectin, a major protein of mineralized bone. Proc. Natl. Acad. Sci. USA. *83*, 6892–6896.

Termine, J.D., Kleinman, H.K., Whitson, S.W., Conn, K.M., McGarvey, M.L., and Martin, G.R. (1981). Osteonectin, a bone-specific protein linking mineral to collagen. Cell *26*, 99–105.

Tyree, B. (1989). The partial degradation of osteonectin by a bone-derived metalloprotease enhances binding to type I collagen. J. Bone Miner. Res. *4*, 877–883.

Vassali, J.D., and Belin, D. (1987). Amiloride selectively inhibits the urokinase-type plasminogen activator. FEBS Lett. *214*, 187–191.

Wrana, J.L., Overall, C.M., and Sodek, J. (1991). Regulation of the expression of a secreted acidic protein rich in cysteine (SPARC) in human fibroblasts by transforming growth factor β. Eur. J. Biochem. *197*, 519–528.

Yablonka-Reuveini, Z. (1989). The emergence of endothelial cell lineage in the chick embryo can be detected by uptake of acetylated low-density-lipoprotein and the presence of von Willebrand factor. Dev. Biol. *132*, 230–240.

Yost, J.C., and Sage, E.H. (1993). Specific interaction of SPARC with endothelial cells is mediated through a carboxy-terminal sequence containing a calcium-binding E-F hand. J. Biol. Chem. *268*, 25790–25796.

Ziche, M., Jones, J., and Gullino, P.N. (1982). Role of prostaglandin E1 and copper in angiogenesis. J. Natl. Cancer Inst. *69*, 475–482.